A Determination of the Solution Conformation of the Nonmammalian Tachykinin Eledoisin by NMR and CD Spectroscopy†

Jennifer C. Wilson, Katherine J. Nielsen, Michael J. McLeish, and David J. Craik*

Victorian College of Pharmacy, Monash University, 381 Royal Parade, Parkville, 3052 Victoria, Australia

Received November 29, 1993; Revised Manuscript Received March 14, 1994®

ABSTRACT: The nonmammalian tachykinin eledoisin was investigated by use of CD and two-dimensional NMR techniques. In aqueous solution the peptide is conformationally averaged, but on addition of 50% trifluoroethanol (TFE) or sodium dodecyl sulfate (SDS) it adopts an α-helical structure. In TFE/H_2O and SDS, residues 6–10 of eledoisin show more conformational order than the terminal regions, which undergo dynamic fraying. A possible turn in the N-terminal "address" region, the putative receptor recognition site of the peptide, is detected by NMR spectroscopy but appears to undergo substantial conformational averaging. The NMR data indicate that the helical central core of eledoisin is better defined in the micellar environment than in TFE; however, partial unfolding via 3_{10} intermediates occurs in both cases. The conformational preference for SDS-bound eledoisin was examined by three-dimensional structure calculations using NMR-derived distance information in simulated annealing calculations.

Eledoisin, a member of the tachykinin family of peptides, was first isolated from the posterior salivary glands of *Eledone muschata* and *Eledone aldrovandi*, which are mollusc species belonging to the octopod *Cephalopoda* (De Marco & Gatti, 1975). Other tachykinins from nonmammalian sources include kassinin and physalaemin. Their pharmacological properties are complex, including powerful vasodilator and hypotensive action and the stimulation of extravascular smooth muscle. The mammalian tachykinins substance P (SP),[1] neurokinin A (NKA), and neurokinin B (NKB) have similar activities and have been more widely studied. The six principal peptides from the tachykinin family are all 10–11 residues in length and possess the same C-terminal sequence, viz., Phe-X-Gly-Leu-Met-NH_2 (Table 1). This is known as the "message" domain, postulated to be responsible for triggering the receptor. The N-terminal region, or "address" domain, varies greatly in amino acid sequence and length and may be responsible for receptor selectivity (Schwyzer, 1987).

The principal receptors for SP, NKA, and NKB are NK-1, NK-2, and NK-3, respectively, although there is a certain degree of cross-specificity (Schwyzer, 1987). While physalaemin shows selectivity for NK-1, its affinity is less than that of its mammalian counterpart, SP. By comparison with the other tachykinins, the affinities of eledoisin and kassinin for mammalian receptors are weak and their selectivities are much less pronounced. It is thought that the "E"-type eledoisin receptor may be a mixture of NK-2 and NK-3 binding sites (Schwyzer, 1987).

The conformational features of the tachykinins which control receptor binding and influence their biological activity are of significant interest, particularly as the selectivity of these peptides for different receptor sites is not fully understood. The conformational preferences of the receptor-specific tachykinins SP, NKA, NKB, and physalaemin have been investigated under a range of conditions by methods including IR, CD, and NMR spectroscopy. There is general agreement that the C-terminal tripeptide, Gly-Leu-Met-NH_2, is folded in methanol (Sumner *et al.*, 1990; Chassaing *et al.*, 1987; Loeuillet *et al.*, 1989), although structure–activity relationship studies on SP suggest that this region should adopt a trans polyproline extended conformation (Loeuillet *et al.*, 1989). There are no discernible trends in the conformations of the "address" segments of these peptides; however, the "message" domains are similar in each case. In general, the "message" domain of these peptides undergoes conformational averaging in aqueous environments (Woolley & Deber, 1987; Sumner *et al.*, 1990; Chassaing *et al.*, 1987). In hydrophobic environments, it assumes conformations variously described as helical (Schwyzer, 1987; Wu & Yang, 1978, 1983; Wu *et al.*, 1982; Woolley & Deber, 1987; Chassaing *et al.*, 1986; Hölzemann, 1989; Horne *et al.*, 1993) or as a series of tight turns in dynamic equilibrium (Sumner *et al.*, 1990). These results may be rationalized in terms of "nascent" helical structures where the folded states are in equilibrium with partially unfolded and extended states as shown below. For many small, linear peptides this equilibrium is biased toward extended and turn-like formations in aqueous solution. The addition of structure-promoting solvents can shift this equilibrium toward helix formation (Osterhout *et al.*, 1989).

$$\text{extended} \rightleftarrows \text{turn} \rightleftarrows 3_{10}\text{-helix} \rightleftarrows \alpha\text{-helix}$$

Few studies have been done on the conformations of the tachykinins eledoisin and kassinin. From CD studies eledoisin has been reported to assume a β-structure, resulting perhaps from aggregation, when in contact with phosphatidyl membranes (Schwyzer, 1987), and to form secondary structure, presumed to be of an α-helical nature in SDS (Woolley & Deber, 1987). In a study of eledoisin in DMSO (Yu & Yang, 1991) by NMR and distance geometry techniques, no preferred conformations were found. This is not surprising since DMSO is generally considered destabilizing to secondary structure

† This work was supported jointly by the Australian Research Council and the Department of Education, Employment and Training.

* Author to whom correspondence should be addressed.

® Abstract published in *Advance ACS Abstracts,* April 15, 1994.

[1] Abbreviations: CD, circular dichroism; NMR, nuclear magnetic resonance; TFE, 2,2,2-trifluoroethanol; SDS, sodium dodecyl sulfate; SP, substance P; NKA, neurokinin A; NKB, neurokinin B; IR, infrared; NOE, nuclear Overhauser effect; NOESY, two-dimensional nuclear Overhauser spectroscopy; TOCSY, total correlation spectroscopy; COSY, two-dimensional correlated spectroscopy; DQF-COSY, double-quantum-filtered COSY; DIPSI, decoupling in the presence of scalar interactions; DSS, 4,4-dimethyl-4-silapentane-1-sulfonate; FID, free induction decay; 2D, two-dimensional; RMSD, root-mean-square deviation; pGlp, pyroglutamic acid.

0006-2960/94/0433-6802$04.50/0

through competition with backbone C=O donor sites for H-bonding to NH protons (Jackson & Mantsch, 1991).

In the current study the secondary structure of eledoisin in a range of solvent conditions has been investigated by CD and ^{1}H NMR spectroscopic methods. The solution structure of eledoisin in a mixture of TFE/H_2O was determined by ^{1}H NMR techniques at 298 K and compared to the results at 278 K. The peptide was also examined in an SDS micellar environment, at 298 K. SDS micelles, aside from the advantage of increasing the effective correlation time of peptides through association, can stabilize α-helical structures in small peptides (Wu *et al.*, 1982; Wu & Yang, 1983; Woolley & Deber, 1987; Mammi & Peggion, 1990). Conformational studies of membrane-binding signal peptides have shown a correlation between micelle-bound conformations and *in vivo* activities, and Rizo *et al.* (1993) proposed that micelles can be used as model membranes and are better mimics of biological membranes than TFE/H_2O mixtures. They suggest that strong association between the hydrophobic helical core of these peptides and the hydrocarbon chains of the SDS micelles is responsible for the enhancement of helix stability.

We have also examined the utility of theoretical structure predictions for determining the preferred conformations of eledoisin. Previous sequence-predictive analyses applied to SP using the method of Chou and Fasman (1974) were equivocal (Wu & Yang, 1978, 1983; Wu *et al.*, 1982) due to the limitations of the algorithm used, which did not take into account the range of conditions a membrane-binding peptide may experience in a biological environment. In the current study, the conformational preferences of the six principal tachykinins have been simulated using the method of Ptitsyn and Finkelstein (1983). This program predicts elements of secondary structure on the basis of the physical properties of polypeptides when they are placed in aqueous, partial hydrophobic, and fully hydrophobic environments.

MATERIALS AND METHODS

Eledoisin (pGPSKDAFIGLM) was obtained from AUSPEP Pty Ltd (Melbourne, Australia).

CD Spectroscopy. CD spectra were recorded on an AVIV 60DS spectropolarimeter. The instrument was calibrated using *d*-10-camphorsulfonic acid. Cells of path length either 0.1 or 0.02 cm were employed and were maintained at a temperature of 15 °C using a Lauda circulating water bath. Peptide concentrations were between 50 μM and 1 mM. Spectra were an average of five scans recorded with a bandwidth of 1 nm, a 0.25-nm step size, and a 0.2-s time constant. Following base-line correction, the observed ellipticity was converted to a mean residue ellipticity (deg·cm^2·dmol^{-1}) using the relationship $[\theta] = \theta \times 1/(lcN)$, where θ is the observed ellipticity, l is the path length in mm, c is the molar concentration, and N is the number of residues in the peptide. The spectra were then smoothed using a third-order polynomial function.

NMR Spectroscopy. Samples for ^{1}H NMR spectra were prepared as follows: eledoisin (2 mM) and SDS-d_{25} (200 mM) in 90% H_2O/10% D_2O, pH 4.4; eledoisin (2 mM) and SDS-d_{25} (200 mM) in 100% D_2O; eledoisin (5 mM) in 50% TFE/H_2O mixture, pH 5.4.

^{1}H NMR experiments were run on Bruker AMX spectrometers operating at 300 and 500 MHz with spectral widths of 3030 and 5050 Hz, respectively. The 2D experiments included DQF-COSY (Rance *et al.*, 1983); NOESY (Kumar *et al.*, 1980) with mixing times of 100 and 250 ms for the micelle sample and 100, 300, and 500 ms for the TFE sample; and TOCSY (Braünschweiler & Ernst, 1983; Davis & Bax, 1985) using a DIPSI spin-lock sequence (Cavanagh & Rance, 1992) with mixing times of 60 and 120 ms. Micelle experiments were run at 298 K; TFE experiments, at 298 and 278 K. Temperature calibration of the probe was achieved by comparison to ethylene glycol chemical shifts. All chemical shifts (ppm) were referenced externally to the methyl resonance of 4,4-dimethyl-4-silapentane-1-sulfonate (DSS, 0 ppm).

Typically, 2D experiments involved 256–400 t_1 increments (800–1000 for DQF-COSY spectra), with 32 transients (80–96 for NOESY spectra) in 2K data points (4K for DQF-COSY spectra), with recycle delays between 1.5 and 2 s for all experiments. Water suppression was achieved by continuous low-power presaturation during the recycle delay for the TOCSY and DQF-COSY spectra and by a combination of a semiselective jump–return sequence (Plateau & Gueron, 1982) and mild presaturation for the NOESY sequence.

Spectra were processed using UXNMR (Bruker) on an X32 data station or by using the FELIX program (Hare Research, Inc.) on a Silicon Graphics 4D/30 Personal Iris workstation. A polynomial function was applied to each FID prior to Fourier transformation to minimize spectral distortions due to the residual water signal, and generally the data were multiplied by a 60° shifted sine-bell window function in each dimension before transformation to produce matrices consisting of 1K × 1K (2K × 2K for DQF-COSY) data points. Some base-line correction on processed spectra was applied around the region of presaturation.

Peak volumes on the 200-ms (100-ms for the TFE data) NOESY spectra were classified as strong, medium, or weak corresponding to upper-bound interproton distance restraints of 2.7, 3.5, and 5.0 Å, respectively (Clore *et al.*, 1986). Appropriate pseudoatom corrections were applied to nonstereospecifically assigned methylene and methyl protons (Wüthrich *et al.*, 1983), and in addition, 1.5 Å was added to the upper limits of distances involving methyl protons. $^3J_{NH\text{-}H\alpha}$ coupling constant ranges were obtained by selecting appropriate slices in the 2D DQF-COSY spectrum, subjecting them to an inverse Fourier transformation, zero-filling to 8K data points, and performing a Hilbert transformation. The distance between antiphase peaks and apparent linewidths was measured, and these values were used with a simple deconvolution routine to estimate coupling constants.

Structure Calculations. Three-dimensional structures were generated from the NOE distance data using the XPLOR software package (Version 3.0; Brünger, 1992). The standard force field and parameter sets of XPLOR were used with minor modifications to deal with the N-terminal pyroglutamic acid residue. An *ab initio* simulated annealing protocol (Nilges *et al.*, 1988), starting from a series of template structures with randomized coordinates, was applied to generate a set of 45 structures. The simulated annealing protocol consisted of 20 ps of high-temperature molecular dynamics with a low weighting on the NOE constraints at 720 K. This was followed by 10 ps of dynamics with an increased weighting on the experimental NOE constraints. The system was then cooled to 100 K over 15 ps, and the structures were subjected to 200 cycles of energy minimization. Structure refinement was achieved by restrained Powell energy minimization using a refined force field, based on the CHARMM program (Brooks *et al.*, 1983). Geometric analysis of the refined structures was performed within XPLOR. Structure superimpositions were accomplished using INSIGHT (Biosym).

Table 1: Amino Acid Sequence, Predicted Secondary Structure, and Helical Content for Tachykinin Peptides in Different Solvent Environments[a-d]

Peptide/environment	Primary sequence/secondary structure prediction[e]											Helical content	
Substance P	Arg	Pro	Lys	Pro	Gln	Gln	**Phe**	Phe	Gly	Leu	**Met-NH_2**		
A				T	T*	T*	*	*				4	(0)[e]
B				T*	T*	T*	h	h	h	h	h	13	(45)
C				h	h	H	H	H	H	H	H	54	(73)
Neurokinin A		His	Lys	Thr	Asp	Ser	**Phe**	Val	Gly	Leu	**Met-NH_2**		
A				T	T	T						1	(0)
B				T	T	T*	*	*	*	*	*	10	(0)
C				*	*	*	H	H	H	H	H	42	(50)
Neurokinin B		Asp	Met	His	Asp	Phe	**Phe**	Val	Gly	Leu	**Met-NH_2**		
A						*	*	*	*	*		5	(0)
B				H	H	H	H	H	H	H	H	68	(90)
C			H	H	H	H	H	H	H	H	H	84	(90)
Physalaemin	Pyr	Ala	Asp	Pro	Asn	Lys	**Phe**	Tyr	Gly	Leu	**Met-NH_2**		
A				T	T*	*	*	*	*	*	*	7	(1)
B			*	h	h	h	h	h	h	h	h	31	(73)
C				h	h	H	H	H	H	H	H	54	(73)
Kassinin	Asp Val	Pro	Lys	Ser	Asp	Gln	**Phe**	Val	Gly	Leu	**Met-NH_2**		
A		T	T	T								3	(0)
B		T	T	T	*	h	h	h	h	h	h	12	(50)
C		T	T	T	*	H	H	H	H	H	H	39	(50)
Eledoisin	Pyr	Pro	Ser	Lys	Asp	Ala	**Phe**	Ile	Gly	Leu	**Met-NH_2**		
A		T	T	T*	*	*	*	*	*			5	(0)
B		T	T	T*	*	h	h	h	h	h	h	19	(55)
C		T	T	T*	*	H	H	H	H	H	H	49	(55)

[a] Residues in boldface highlight regions of homology. [b] Predictions carried out using the program ALB (Ptitsyn & Finkelstein, 1983). [c] T = turn predicted; H = helix predicted; h = helix possible; * = helix not predicted. [d] A, B, and C refer respectively to predictions based on unfolded peptides in H_2O, based on peptide chains being partly immersed in lipid, and based on peptide chains deeply immersed in lipid. [e] Numbers beside predictions refer to the percent helix in fluctuating secondary simulation, and those in parentheses refer to the percent helix in a hypothetical fixed peptide.

RESULTS

Structure Prediction. Table 1 shows secondary structure predictions for the six principal tachykinin peptides using the program ALB (Ptitsyn & Finkelstein, 1983). Also indicated are the helix contents based on fluctuating and fixed secondary structure simulations. No helix formation for any of the peptides is predicted in an aqueous environment, but the "message" domains become increasingly helical as the hydrophobicity is increased. NKB has the greatest helical tendency, with helix predicted over most of the molecule, even when the peptide is only partially immersed in a lipid environment, while NKA shows the lowest helical propensity.

With the exception of NKB, all of the peptides show a propensity for turn formation in their respective "address" domains in aqueous solution. This tendency is retained only for eledoisin and kassinin as the environment becomes progressively lipophilic. This represents an important difference, since eledoisin and kassinin have significantly lower receptor affinities than the remaining peptides in the group and bind to both NK-2 and NK-3 sites (Schwyzer, 1987). Although NKB is not predicted to adopt a turn in hydrophobic conditions, it is predicted to be helical over the corresponding region where turns are predicted in eledoisin and kassinin. This indicates that a folded conformation preceding the message domain may be a prerequisite for NK-3 receptor selectivity.

CD Spectroscopy. Figure 1 shows CD spectra of eledoisin at 288 K in water, 25% and 50% TFE, and SDS micelles (200 mM). The spectrum in water is consistent with the peptide adopting a predominantly random coil conformation (Woody,

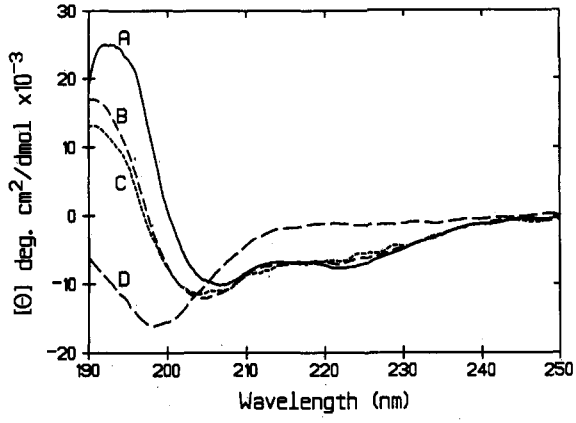

FIGURE 1: CD spectra for eledoisin in H_2O (curve D), 25% (C) and 50% TFE (B), and 200 mM SDS micelles (A) at 288 K.

Table 2: CD Determination of α-Helix Content and Helical Parameters $R1$ and $R2$ for Eledoisin[a]

solvent	$[\theta]_{222}$[b]	PROSEC[c]	polylysine[d]	$R1$[e]	$R2$[e]
H_2O	3.6	0.0	7.5	0.81	0.07
25% TFE	21.7	10.6	24.9	−1.15	0.57
50% TFE	23.2	13.1	28.3	−1.41	0.58
200 mM SDS	25.3	22.2	23.4	−2.45	0.75

[a] CD data were collected at 15 °C at peptide concentrations between 50 μM and 1 mM. [b] Calculated using the method of Chen *et al.* (1974). [c] Calculated by fitting data to reference spectra of Yang *et al.* (1986). [d] Calculated by fitting data to the polylysine spectra of Greenfield and Fasman (1969). [e] Helical parameters $R1$ and $R2$ calculated as described in Bruch *et al.* (1991).

1985). Further, the spectrum remains essentially unchanged when the peptide concentration is varied from 50 μM to 1 mM (data not shown), indicating that aggregation, if any, has no effect on peptide conformation.

Addition of TFE induces a shift toward a helical conformation. At 50% TFE the minimum has shifted from 198 to 205 nm ($\pi\pi^*$-transition) and considerable negative ellipticity has developed at 222 nm ($n\pi^*$-transition). The shift toward a helical structure in a hydrophobic environment is accentuated in SDS with mimima arising at 207 and 222 nm.

If it is assumed that the absorption at 222 nm is almost exclusively due to α-helix (Woody, 1985), it is possible to calculate the α-helicity using the equation of Chen *et al.* (1974):

$$[\theta]_\lambda = (f_H - ik/N)[\theta]_{H\lambda\infty}$$

where $[\theta]_\lambda$ is the observed mean residue ellipticity at wavelength λ, f_H is the fraction of helix, i is the number of helical segments (1 for eledoisin), k is a wavelength-dependent constant, and $[\theta]_{H\lambda\infty}$ is the maximum mean residue ellipticity for a helix of infinite length. On this basis, the $[\theta]_{222}$ for eledoisin in a 100% helical conformation was calculated to be −30 300 deg·cm²·dmol⁻¹. Thus, at 15 °C, the population averages of helical conformations in water, 50% TFE, and SDS were approximately 4%, 23%, and 25%, respectively (Table 2).

For a comparison with the results obtained from $[\theta]_{222}$ data we used the curve fitting program PROSEC (Aviv Co.) to estimate secondary structure. This program is based on the algorithm and basis spectra of Yang *et al.* (1986) and provides an estimate of α-helix, β-sheet, β-turn, and random coil. As seen in Table 2, the predicted trend toward higher helicity in more hydrophobic environments is similar to that seen from the $[\theta]_{222}$ data, but the absolute values for helical content are somewhat lower. Fitting the data to reference polylysine

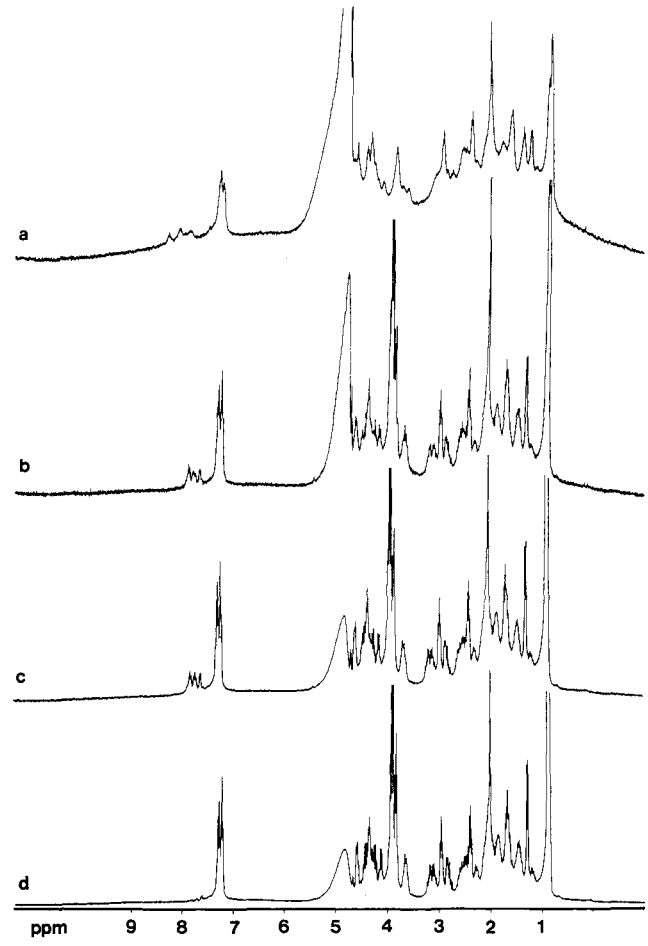

FIGURE 2: (a) ^{1}H NMR spectrum of eledoisin (2 mM) in D_2O. (b–d) Spectra after addition of successive aliquots of trifluoroethanol-d_3 (TFE) (298 K, 300 MHz): (b) 23% TFE, (c) 28% TFE, (d) 33% TFE.

spectra (Greenfield & Fasman, 1969) also exhibited the same trend, but again, absolute values varied considerably.

This variation in helical content calculated by the different methods is not unusual. In a recent paper, Bruch *et al.* (1991) describe the difficulty in estimating helicity using the above methods, citing problems with inaccuracies in determining peptide concentrations as well as those caused by small shifts in wavelength. Instead, for comparisons of closely related peptides, they suggest using two parameters, $R1$ and $R2$, which are independent of wavelength shifts and peptide concentration. $R1$ is defined as the ratio of the intensity of the maximum between 190 and 195 nm and the intensity of the minimum between 200 and 210 nm. $R2$ is the ratio of the intensity of the minimum near 222 nm and the intensity of the minimum between 200 and 210 nm (Bruch *et al.*, 1991). For a random coil, $R1$ is positive and $R2$ is close to zero. As the helicity increases, $R1$ will be close to −2 and $R2$ will approach 1 (Bruch *et al.*, 1991; Rizo *et al.*, 1993). As can be seen from Table 2, the $R1$ and $R2$ values demonstrate that eledoisin adopts a helical conformation in a hydrophobic environment. However, it is more obvious from these data that the greatest helicity is observed in SDS micelles.

^{1}H NMR Spectroscopy. (A) Eledoisin in H_2O. Figure 2a shows a 300-MHz ^{1}H NMR spectrum of eledoisin in D_2O. Two notable features are the broadness of the peaks, which indicates the presence of aggregation, and the fact that some NH protons remain unexchanged more than 1 h after dissolution in D_2O. This protection from solvent accessibility is most likely also a function of the aggregated state. Addition

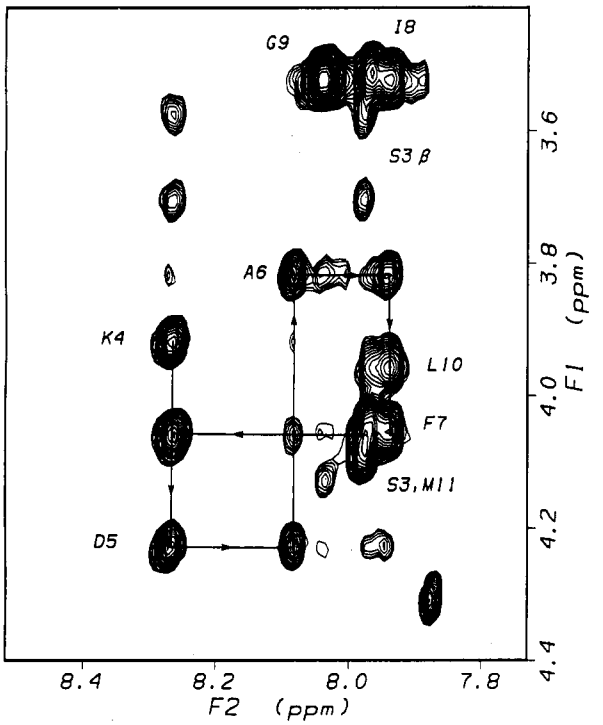

FIGURE 3: Portion of the 100-ms NOESY spectrum (500 MHz) of eledoisin (2 mM, 50% TFE/H_2O, 278 K) showing the αH–NH region with sequential connectivities.

of TFE (Figure 2b–d) causes sharpening of the peaks, and a concomitant increase in the rate of amide exchange, both indicative of deaggregation of the peptide. TFE is known to enhance helix formation in peptides with inherent propensities toward helix formation (Sönnichsen *et al.*, 1992; Nelson & Kallenbach, 1989). In view of its favorable structure-promoting and deaggregating properties, TFE was considered a suitable medium for the 2D ^1H NMR study of eledoisin. No further NMR work was carried out in H_2O because of the peptide aggregation and, also, since the CD results indicated that eledoisin is unstructured in aqueous media.

(B) Eledoisin in TFE/H_2O. (1) Chemical Shift Assignments. ^1H resonance assignments were achieved using two-dimensional NMR techniques (Wüthrich, 1986). TOCSY and DQF-COSY experiments were used to identify the spin systems of individual amino acid residues. As each of the amino acids is unique within the sequence, assignment was straightforward. Nevertheless, to check for consistency of the data, the sequential connectivity pathway linking the αH of each residue with the NH of the next was identified by reference to NOESY spectra. Those recorded at 298 K and 300 MHz lacked cross-peaks, even when very long mixing

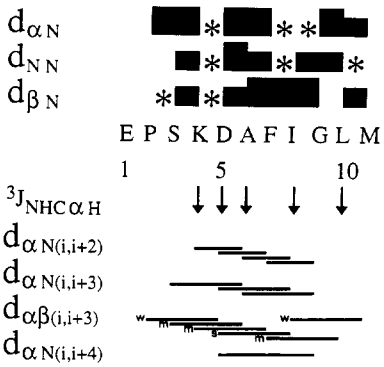

FIGURE 4: Schematic diagram showing the intensity of NOE connectivities (filled bars) between the backbone amide and αH protons observed for eledoisin (2 mM, 50% TFE/H_2O, 278 K). NOE intensities are given as either strong, medium, or weak. Asterisks indicate that overlapped peaks precluded definitive confirmation of the NOE. Arrows indicate coupling constants less than 6 Hz.

times (800 ms) were employed. Lowering the temperature to 278 K sufficiently increased the correlation time, τ_c, of the peptide to the point where all sequential and several medium-range connectivities were observable at short mixing times (100 ms), especially at higher field. Figure 3 shows the sequential assignment pathway traced on the αH–NH region of the 100-ms NOESY spectrum recorded in 50% TFE at 278 K and 500 MHz. There is considerable overlap, particularly for the serine, methionine, leucine, and phenylalanine residues, but the assignments are unambiguous because of the lack of degenerate residue types. Chemical shifts are summarized in Table 3.

(2) Coupling Constant and Slow Exchange Data. All measurable $^3J_{NH\text{-}\alpha H}$ coupling constants from residues 4–10 were in the range 5–6.5 Hz. These low values indicate that extended structures, whose $^3J_{NH\text{-}\alpha H}$ values are expected to exceed 8.5 Hz, were not present to any significant extent for these residues. While the coupling constants are not as low as would be expected for well-defined α-helices, the susceptibility of short, linear peptides to undergo conformational averaging is well-known (Dyson & Wright, 1991). At least three NH protons remained observable up to 45 min after the addition of TFE to a 2 mM solution of eledoisin in D_2O, suggesting that there is some protection from solvent exposure. These protons could not be unambiguously assigned because of severe overlap in the NH region of the spectrum.

(3) NOE Data. A summary of the interresidue sequential and medium-range NOEs is provided in Figure 4. The presence of several NH–NH connectivities, together with αH–NH_{i+3} and αH–βH_{i+3} connectivities, suggests that some helical elements are present. Overlap in the αH–NH region interfered with the NOE analysis; however, the number of αH–βH_{i+3}

Table 3: 500-MHz ^1H Resonance Assignments[a] for Eledoisin (2 mM) in 50% TFE/H_2O, 278 K

residue	NH	CαH	CβH	other
pGlu-1		4.52	2.53, 2.05	
Pro-2		4.32	2.21, 1.86	CγH 1.93, 2.01; CδH 3.60, 3.92
Ser-3	7.82	4.26	3.79, 3.92	
Lys-4	8.10	4.14	1.82, 1.76	CγH 1.40; CδH 1.61; CεH 2.88; εNH$_3$ 7.55
Asp-5	8.11	4.45	2.72	
Ala-6	7.92	4.04	1.26	
Phe-7	7.78	4.28	3.15, 3.05	$H_{2,6}$ 7.11; $H_{3,4,5}$ 7.23
Ile-8	7.80	3.70	1.81	$CH_3\gamma$ 0.81; $CH_3\delta$ 0.81; $CH_2\gamma$ 1.15, 1.54
Gly-9	7.90	3.74		
Leu-10	7.77	4.18	1.49, 1.67	CγH 1.72; $CH_3\delta$ 0.78, 0.82
Met-11	7.81	4.25	1.88, 1.93	CγH 2.25, 2.34; SCH_3 2.01
terminal NH_2	7.21, 6.86			

[a] Chemical shifts are given in ppm and are relative to the DSS peak (0 ppm).

NOEs observed in the less crowded aliphatic region of the spectrum indicates that eledoisin is substantially folded from residues 2 to 11. The presence of some population of α-helix is supported by the observation of an αH–NH$_{i+4}$ connectivity between residues 5 and 9, but the relative strengths of the sequential NOEs, particularly near both termini, are not representative of a well-defined α-helix. Similarly, the observation of an αH–NH$_{i+2}$ connectivity between residues 5 and 7 is more consistent with a 3_{10}-helix than an α-helix. The simultaneous observation of these various types of NOEs suggests that some degree of conformational averaging is present, based around a predominantly helical core. It is noteworthy that some distortion occurs around Asp-5, since Asp residues are considered to be helix destabilizing (Ptitsyn & Finkelstein, 1983) and are often found at the N-cap positions of regular helices and, more commonly, at the N-cap position of 3_{10}-helices (Karpen *et al.*, 1992). At longer mixing times ($\geq$300 ms) several more αH–NH$_{i+2}$ NOEs are present (Figure 4); however, these are accompanied by other cross-peaks (*i.e.*, αH–NH$_{i-1}$) which presumably result from spin diffusion.

The weakness of the αH–βH$_{i+3}$ connectivities at both ends of the peptide may be explained by dynamic fraying and/or turn formations at the helix termini. At the amidated C-terminus, the observation of a medium-range NOE between one of the amide NH$_2$ protons and the αH protons of Gly-9 suggests that any regular α-helix in this region is in equilibrium with 3_{10}-helix or turnlike conformations. The possibility of turn conformations must be considered for the region near the N-terminus since any helix involving residues 2–5 is likely to be unstable due to the helix-breaking tendencies of Asp, Ser, and Pro residues (Ptitsyn & Finkelstein, 1983). Sönnichsen *et al.* (1992) report that TFE does not induce helix independently of sequence and that helix-stop signals are recognized. Consequently, the weak αH–βH$_{i+3}$ connectivities observed could arise from a turn immediately preceding the helix. Overlap prevented confirmation of the presence of such a turn, which could have been achieved by the observation of $i + 2$ connectivities in this region.

(C) Eledoisin in SDS Micelles. (1) Chemical Shift Assignments. Assignment of the proton resonances of eledoisin in SDS micelles was achieved using the procedure described for the TFE experiments. The αH–NH region of the NOESY spectrum of SDS-bound eledoisin (Figure 5) is significantly more dispersed than the spectrum of eledoisin in 50% TFE/H$_2$O. Chemical shift data are given in Table 4. It is interesting to note that the TOCSY spectra for eledoisin in SDS showed complete NH to side-chain correlations for all residues. It is not unusual for peptide/micelle systems to give poor TOCSY spectra (McLeish *et al.*, 1993; Rizo *et al.*, 1993) due to the high molecular weight of the micellar aggregate, so the high-quality spectra obtained for eledoisin/SDS may reflect a more facile averaging between free and micelle-bound states for eledoisin compared with other peptides.

(2) Coupling Constant and Slow Exchange Data. For eledoisin in SDS micelles, the measurement of $^3J_{\text{NH-H}\alpha}$ coupling constants was unreliable due to the particularly broad linewidths, but approximate ranges were derived. Coupling constants for residues 4–7 were unequivocally established to be less than 6.5 Hz, suggesting that extended structures are not present to any significant extent. To detect and identify "slow exchange" NH backbone protons, a TOCSY spectrum of a freshly prepared solution of eledoisin in D$_2$O/SDS was run, commencing approximately 30 min after dissolution. Amide protons Phe-7 to Met-11 were detected in this TOCSY spectrum, indicating that these protons exchange slowly with

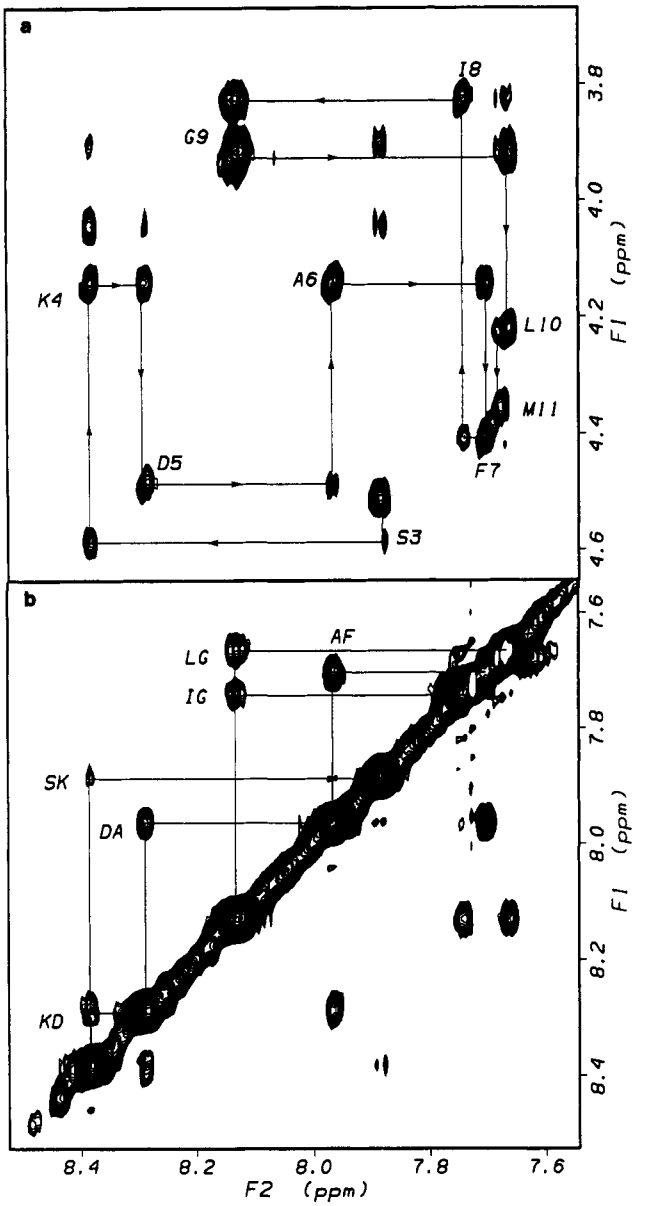

FIGURE 5: Portion of the 250-ms NOESY spectrum (500 MHz) of eledoisin (2 mM, 200 mM SDS, 90% H$_2$O/10% D$_2$O, 298 K) showing (a) the αH–NH region with connectivities and (b) the amide region with $d_{\text{NN}}(i,i+1)$ NOE connectivities.

the D$_2$O solvent, probably as a result of their participation in hydrogen bonds. The slow exchange data provide information on the possible length of helix for eledoisin in SDS. Since the NH proton of the fifth residue forms an H-bond with the carbonyl oxygen of the first residue of a regular α-helix, then for eledoisin any α-helix would stretch from residues 3 to 11, or from residues 4 to 11 for 3_{10}-helix.

(3) NOE Data. A summary of sequential and medium range NOE connectivities is given in Figure 6. A series of strong and medium-strength sequential NH–NH connectivities is observed from residues 4 to 11, suggestive of a folded structure. By comparison with the TFE data, the relative strengths of the sequential NOEs along the central region of eledoisin (*i.e.*, residues 5–10) are more representative of a well-defined helix. Several αH–NH$_{i+3}$ and αH–βH$_{i+3}$ NOE cross-peaks are observed along the stretch 4–11. However, they are accompanied by several αH–NH$_{i+2}$ cross-peaks, suggesting partial unfolding via 3_{10}-helix intermediates. In support of this, the strengths of some of the αH–βH$_{i+3}$ connectivities are slightly weaker than would be expected for a regular α-helical

Table 4: 500-MHz ^{1}H Resonance Assignments[a] of Eledoisin (2 mM) and SDS-d_{25} (200 mM) in 10% D_2O/90% H_2O, 298 K

residue	NH	CαH	CβH	other
pGlu-1		4.62	2.52, 2.07	CγH 2.36
Pro-2		4.44	2.23, 1.84	CγH 1.96; CδH 3.72, 3.53
Ser-3	7.79	4.52	3.82, 3.97	
Lys-4	8.31	4.07	1.84	CγH 1.43; CδH 1.88; CϵH 2.95; NH_3^+ 7.62
Asp-5	8.21	4.42	2.72	
Ala-6	7.89	4.34	1.27	
Phe-7	7.63	4.34	3.03, 3.15	H_ϕ 7.16
Ile-8	7.68	3.75	1.85	$CH_3\gamma$ 0.86; $CH_3\delta$ 0.86; $CH_2\gamma$ 1.20, 1.54
Gly-9	8.04	3.80		
Leu-10	7.58	4.15	1.55, 1.71	CγH 1.71; $CH_3\delta$ 0.84, 0.89
Met-11	7.58	4.28	1.95, 2.06	CγH 2.35, 2.45; SCH_3 1.93
terminal NH_2	6.83, 7.11			

[a] Chemical shifts are given in ppm and are relative to the DSS peak (0 ppm).

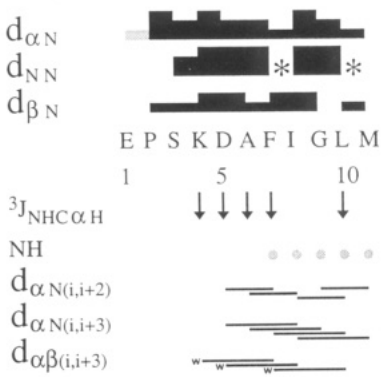

FIGURE 6: Schematic representation of NOE connectivities for eledoisin (2 mM, 200 mM SDS, 90% H_2O/10% D_2O, 298 K). NOE intensities are given as either strong, medium, or weak. Asterisks indicate that NOEs were not confirmed due to overlap.

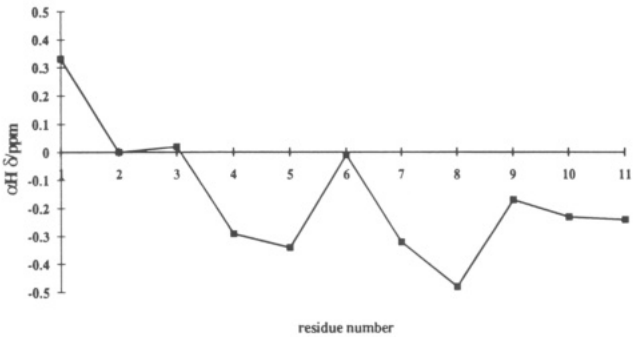

FIGURE 7: Graph of αH chemical shift deviations from random coil values for eledoisin in SDS micelles. The error in the measured chemical shift values is 0.02 ppm.

structure, and no αH–NH_{i+4} connectivities are observed. The αH–NH_{i+2} cross-peak from Ile-8 to Leu-10 is stronger than its αH–NH_{i+3} counterpart, indicating that the folded C-terminus is 3_{10}-like in character. This is supported by the medium-strength αH–NH_{i+2} cross-peak between Gly-9 and Met-11.

The region preceding Asp-5 is less defined than the latter segments, judging by the lack of αH–NH_{i+2} and αH–NH_{i+3} connectivities and the weakness of the αH–βH_{i+3} connectivity observed between Lys-4 and Phe-7. Some degree of conformational order is inferred by a medium-strength NH–NH_{i+1} NOE between Ser-3 and Lys-4, an i+2 NOE from one of the Ser βH protons to the NH of Asp-5, and a weak NH–NH_{i+3} NOE between Ser-3 and Ala-6. The latter two connectivities are not representative of a helix structure and may arise from a turn preceding the helical core. The absence of an αH–NH_{i+2} connectivity suggests that any turn in this region is ill-defined. Although the possibility of a turn incorporating residues 2–5 is inconsistent with the estimate of helix length deduced from the slow exchange experiments, the polar side chains of residues such as Asp and Ser, when preceding helices, can provide stabilizing C=O donors for H-bond interactions in helices (Karpen *et al.*, 1992). This type of interaction may be especially important for the stabilization of short lengths of helix in small, linear peptides.

(4) Estimations of Percentage of Folded Conformations of Eledoisin. Estimates of the fraction of molecules possessing folded conformations can be obtained both by the analysis of αH–NH_{i+1} and NH–NH NOE intensities using the procedure of Bradley *et al.* (1990) and by analysis of αH chemical shift deviations from random coil values using the method of Rizo *et al.* (1993). In these analyses, we use the term "folded" in preference to "helix" since reverse turn and helix structures can produce similar NOE intensities and αH chemical shifts and, in the case of eledoisin, the equilibrium of conformers is more complex than that of a two-state model.

Figure 7 shows αH chemical shift deviations for eledoisin in SDS. These αH shifts are significantly upfield from random coil values, suggesting the presence of helical conformations. Quantitative analysis of these data shows that the prevalence of folded structures is 45%, when calculated over the whole sequence, or 76% over residues 4–11. While the value of 45% is somewhat higher than that indicated by the CD data, this may be rationalized by potential difficulties in the CD spectra of small peptides, where dichroism of aromatic amino acids can mask the CD signal of "structured" conformers, especially for short helices. Small deviations from ideal helical geometry and dynamic fraying of helix termini will further contribute to lowering of ellipticity values in the CD signal (Dyson & Wright, 1991). An important advantage of the NMR method is that it provides residue-specific information on conformation, and the result that 76% of conformers over the residues 4–11 are structured is an important one. Calculations based on NOE intensities (Bradley *et al.*, 1990) confirmed a similarly high helical content (averaging >90%) over these residues. The higher estimate from the NOE data most likely reflects the fact that the observed NOEs are weighted predominantly toward the SDS-bound state. Under the conditions examined, both free and bound eledoisin are present in solution, but the effective molecular weight of the micelle-bound species leads to more rapid buildup of NOEs. As the free peptide is likely to be unstructured, techniques such as CD which yield averages over all contributing forms will lead to lower estimates of structured forms.

In summary, the NMR information is consistent with the presence of an α-helix in equilibrium with 3_{10}-helix, at least along the central core of eledoisin. Some unfolded species are present in TFE and, to a lesser extent, in SDS-bound eledoisin.

Table 5: Comparison of Refinement Protocols Involving Different H-Bond Arrangements[a]

structures	degree of convergence	av no. of NOE violations >0.1 Å		NOE energy (kcal/mol)
		A[b]	B[c]	
no H-bond	20/20	1.9	1.9	1.7
α-helix (6–11)	16/20	4.3	6.3	3.9
3_{10}-helix (6–11)	19/20	2.9	3.2	3.3

[a] Refined structures were calculated for a set of 20 structures chosen randomly from the primary structures. [b] Calculated for converged structures. [c] Calculated for all structures.

The C-terminus displays 3_{10}-helix- or turn-like characteristics, whereas the segment 2–5, while showing some degree of order, is not unambiguously defined in either TFE or SDS.

(5) Three-Dimensional Structure of Eledoisin. While caution must be exercised in attempting to calculate a solution structure when there are indications of conformational averaging, the high fraction of folded conformers indicated in the SDS-bound NOE data suggested that an accurate representation of the structures would be obtained from simulated annealing calculations using observed NOEs to generate distance constraints. An initial set of 45 structures was calculated using a total of 123 distance constraints derived from 76 intraresidual, 32 sequential, and 15 medium-range NOEs. All simulated annealing runs converged to give a single family of structures. These were calculated without the explicit inclusion of H-bonds. Although a number of moderately slowly exchanging NH protons are present, it was not possible to unambiguously identify their H-bonding partners in the preliminary set of structures. It was therefore decided to complete the structure refinement process in triplicate to compare alternative possible H-bonding arrangements. Three sets of 20 refined structures were generated from randomly chosen structures of the preliminary set. In the first set, no H-bonds were included in the refinement. In the second set, H-bonds were added as distance constraints between the NH protons of residues 8–11 and the C=O oxygens four residues earlier in the sequence, as would occur in a regular α-helix. A third set of structures was refined under the influence of $C{=}O_i$, NH_{i+3} H-bond constraints appropriate for 3_{10}-helical structures. It was of interest to see if either type of helix dominates the structural equilibrium by a comparison of the residual NOE violations among the three sets. A summary of various energy and NOE-violation terms for the three sets is given in Table 5.

A superimposition of the first set of refined structures (Figure 8) in which no H-bonding assumptions are made shows a helical region which is reasonably well-defined. The backbone pairwise RMSD for all residues is 1.44 Å, with a standard deviation of 0.59 Å. Figure 9 shows the atomic RMS distribution of the 20 structures about the mean structure for the backbone atoms and all atoms, respectively. The lowest RMS differences are seen for residues 4–9, where the folded structures determined from the NOE data are best defined. The generally good fit of the derived structures to the NMR constraints shows that the assumption of the NOEs being interpreted in terms of a predominant set of structures is reasonable.

An analysis of the Φ–Ψ combinations for all 20 structures shows that residues 6–11 are well-defined in the α-region of the Ramachandran plot. Measurements of $C{=}O_i$, NH_{i+3} versus C=O, NH_{i+4} distances along the stretch 5–11 were made, and the $i,i+3$ distances were less than 3.0 Å in the majority (>75%) of structures whereas $i,i+4$ distances were less than 3.0 Å in only 50% of structures, with many distances being greater than 4.0 Å. This suggests that eledoisin has a preference for 3_{10}-helix over regular helix.

Analysis of convergence, energy, and NOE violations for refined structures derived using the three sets of H-bonding patterns (Table 5) confirms the preference for 3_{10}-helix over regular helix. The average number of NOE violations per structure for the regular helix set is significantly greater than those for the set of 3_{10}-helix structures. Furthermore, the rate of nonconvergence is much higher for the regular helix structures than for either of the 3_{10}-helical or non-H-bonded cases. Note that the increased NOE violations and energies of structures caused by the addition of H-bond constraints is a reflection of the fact that the observed NOEs represent time-averaged populations and that minor populations of unfolded species are present in the solution equilibrium.

FIGURE 8: Stereoview showing the superimposition of the backbones of the final 20 simulated annealing structures (residues 4–9) of eledoisin in SDS micelles.

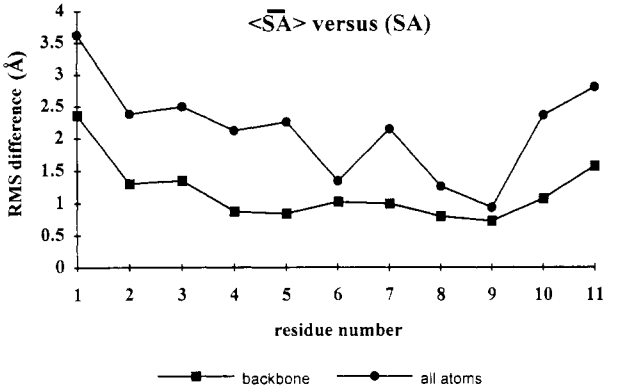

FIGURE 9: Atomic RMS distribution of the 20 final simulated annealing run structures about the mean structure for the backbone atoms and all atoms.

The region encompassed by residues 1–5 was also examined by analysis of the Φ–Ψ dihedral combinations in structures calculated without H-bond constraints. The relationship between pGlp-1 and Pro-2 is limited to the conformational space available in polyproline conformations due to the proline-like nature of the pyroglutamate. An extended polyproline conformation is adopted in most structures for pGlp-1 (17/20) and for Pro-2 (20/20). The Φ–Ψ angles of Ser-3 are scattered just outside the α-region of the Ramachandran plot, indicating that some unfolding occurs at this residue. The dihedral angles for Lys-4 and Asp-5 are within the α-region. The αH_i–αH_{i+3} distances between Pro-2 and Asp-5 are within 7.0 Å in 18/20 structures. This distance is the threshold commonly used to define a β-turn, provided the central regions are not helical (Lewis *et al.*, 1973). However, it is not appropriate to interpret the data for this region in terms of a single turn conformation. The likely situation is that eledoisin exists in equilibrium between two states, *i.e.*, one in which a type I β-turn over residues 2–5 is followed by a stretch of predominantly 3_{10}-helix from 6 to 11, and another where the helical region extends from residues 3 to 11. Extension of the helix toward the N-terminus past Asp-5, which is often found in the N-cap position of 3_{10}-helices, is consistent with the recent findings of Li and Deber (1993) that classical helix-breaking residues in globular proteins can often be accommodated in helices in membrane-mimetic environments.

DISCUSSION

Eledoisin aggregates and undergoes extensive conformational averaging in water, but is in a monomeric, structured state in the presence of TFE or SDS micelles. The NMR studies reported here suggest that, in hydrophobic environments, part of the "address" domain and the whole of the "message" domain of eledoisin are folded. In SDS, the structural equilibrium is biased toward a 3_{10}-helix from residues 6 to 11. Small populations of regular α-helix (and unfolded conformations) cannot be excluded in the solution ensemble since 3_{10}-helices are intermediates in the folding/unfolding pathway of α-helices (Tirado-Rives & Jorgensen, 1991; Sundaralingham & Sekharudu, 1989). The change in H-bonding from *i*,*i*+4 to *i*,*i*+3 interactions does not require high energy or specific interactions with "chaperone" molecules (Perczel *et al.*, 1992). Although the environments provided by SDS and TFE are considered favorable for α-helix formation, eledoisin may be too short to sustain a well-defined regular helix *in vitro*. In support of this, NMR data for physalaemin in methanol (Chassaing *et al.*, 1986) were also explained in terms of an equilibrium between α-helix and 3_{10}-helix.

The amidated C-terminus of eledoisin in both TFE and SDS comprises 3_{10}- or turn-like elements, and according to the structures derived from SA calculations on the SDS data, this is accompanied by dynamic fraying of the helix terminus. Although, dynamic fraying of helix termini is expected for small, linear peptides, this observation is interesting in the light of SAR experiments (Glowinski *et al.*, 1987) showing that a certain degree of flexibility at the C-terminus is required for binding to neurokinin receptors.

The "address" segment of eledoisin, while undergoing greater conformational averaging than does the "message" domain, also retains some conformational order in both SDS and TFE. This order may be interpreted as a loosely defined turn, or an unstable continuation of the 3_{10}-helix observed along the "message" domain. SDS micelles, like TFE, enhance helix stability only in cases where the peptide shows a propensity for helix formation, or when the preference for β-structures and helical structures is equivocal (Wu & Yang, 1978; Wu *et al.*, 1982). However, the stability of turns is not known since there are few reported instances of turns occurring in these environments (Sönnichsen *et al.*, 1992; Shin *et al.*, 1993). Whatever the case, the identification of a folded conformation in this segment under hydrophobic conditions is significant, since it may represent an essential feature of NK-2/NK-3 binding.

Secondary structure predictions for eledoisin using the program ALB correlate well with the experimental ^{1}H NMR and CD results. This suggests the program will be useful for application to the other neurokinin peptides. For example, NMR studies of SP, physalaemin, and NKA indicate that "message" domain of these peptides is conformationally averaged in aqueous solution (Sumner *et al.*, 1990; Chassaing *et al.*, 1987). Although NKA exhibits some conformational order at the N-terminus, stabilized by a postulated salt bridge between the side chains of Lys-2 and Asp-4 (S. Sumner, personal communication), Horne *et al.* (1993) have found no evidence for this in a hydrophobic (28% TFE) environment. NKA is predicted to have a turn near the N-terminus only in an aqueous environment. The structure predictions (Table 1) also indicate that, unlike the other neurokinins, NKA requires a full hydrophobic environment to invoke helical folding in the "message" domain. This prediction is confirmed by CD analysis where NKA is shown to have less helix in SDS micelles than SP (Hölzemann, 1989; Wu *et al.*, 1982; Woolley & Deber, 1987), and by NMR where Horne *et al.* (1993) observed that the helical core of NKA undergoes extensive time-averaging. On the basis of the structure predictions and theoretical percent helix calculations, kassinin may be expected to behave in a similar manner to eledoisin. Although this is certainly observed in biological assays of the two peptides (Erspamer *et al.*, 1980; Iversen, 1982), a conformational study of kassinin needs to be undertaken before a true comparison can be made.

ACKNOWLEDGMENT

Bruker Australia is thanked for the generous donation of spectrometer time. Jeff Dyason, Richard Ford, and David Smith are thanked for their assistance with the computational aspects of this study. Prof. Mike Doughty (University of Kansas) is thanked for help with the CD studies.

REFERENCES

Bradley, E. K., Thomason, J. F., Cohen, F. E., Kosen, P. A., & Kuntz, I. D. (1990) *J. Mol. Biol. 215*, 607–622.

Braünschweiler, L., & Ernst, R. R. (1983) *J. Magn. Reson. 53*, 521–528.
Brooks, B. R., Bruccoleri, R. E., Olafson, B. D., States, D. J., Swaminathan, S., & Karplus, M. (1983) *J. Comput. Chem. 4*, 187–217.
Bruch, M. D., McKnight, C. J., & Gierasch, L. M. (1991) *Proteins: Struct., Funct., Genet. 10*, 130–139.
Brünger, A. T. (1992) XPLOR Manual, Yale University, New Haven, CT.
Cavanagh, J., & Rance, M. (1992) *J. Magn. Reson. 96*, 670–678.
Chassaing, G., Convert, O., & Lavielle, S. (1986) *Eur. J. Biochem. 154*, 77–85.
Chassaing, G., Convert, O., & Lavielle, S. (1987) in *"Peptides 1986": Proceedings of the 19th European Peptide Symposium* (Theodoropoulos, D., Ed.) pp 301–306, de Gruyter, Berlin.
Chen, Y.-H., Yang, J. T., & Chau, K. H. (1974) *Biochemistry 13*, 3350–3359.
Chou, P. Y., & Fasman, G. D. (1974) *Biochemistry 13*, 211–221.
Clore, G. M., Brünger, A. T., Karplus, M., & Gronenborn, A. M. (1986) *J. Mol. Biol. 191*, 523–551.
Davis, D. G., & Bax, A. (1985) *J. Magn. Reson. 64*, 533–535.
De Marco, A., & Gatti, G. (1975) *Int. J. Peptide Protein Res. 7*, 437–444.
Dyson, H. J., & Wright, P. E. (1991) *Annu. Rev. Biophys. Biophys. Chem. 20*, 519–538.
Erspamer, G. F., Erspamer, F., & Picinelli, D. (1980) *Naunyn-Schmeideberg's Arch. Pharmacol. 311*, 61–65.
Glowinski, J., Torrens, Y., Saffroy, M., Bergström, L., Beaujouan, J. C., Lavielle, S., Ploux, O., Chassaing, G., & Marquet, A. (1987) *Prog. Brain Res. 72*, 197–203.
Greenfield, N., & Fasman, G. D. (1969) *Biochemistry 8*, 4108–4116.
Hölzemann, G. (1989) *Kontakte (Darmstadt) 2*, 4–11.
Horne, J., Sadek, M., & Craik, D. J. (1993) *Biochemistry 32*, 7406–7412.
Iversen, L. L. (1982) *Br. Med. Bull. 38*, 277–282.
Jackson, M., & Mantsch, H. M. (1991) *Biochim. Biophys. Acta 1078*, 231–235.
Karpen, M. E., de Haseth, P. L., & Neet, K. E. (1992) *Protein Sci. 1*, 1333–1342.
Kumar, A., Ernst, R. R., & Wüthrich, K. (1980) *Biochem. Biophys. Res. Commun. 95*, 1–6.
Lewis, P. N., Momany, F. A., & Scheraga, H. A. (1973) *Biochim. Biophys. Acta 303*, 211–229.
Li, S., & Deber, C. M. (1993) *J. Biol. Chem. 268*, 22975–22978.
Loeuillet, D., Convert, O., Lavielle, S., & Chassaing, G. (1989) *Int. J. Peptide Protein Res. 33*, 171–180.
Mammi, S., & Peggion, E. (1990) *Biochemistry 29*, 5265–5269.
McLeish, M. J., Nielsen, K. J., Wade, J. D., & Craik, D. J. (1993) *FEBS Lett. 315*, 323–328.
Nelson, J. W., & Kallenbach, N. R. (1989) *Biochemistry 28*, 5256–5261.
Nilges, M., Gronenborn, A. M., Brünger, A. T., & Clore, G. M. (1988) *Protein Eng. 2*, 27–38.
Osterhout, J. J., Jr., Baldwin, R. L., York, E. J., Stewart, J. M., Dyson, H. J., & Wright, P. E. (1989) *Biochemistry 28*, 7059–7064.
Perczel, A., Foxman, B. M., & Fasman, G. D. (1992) *Proc. Natl. Acad. Sci. U.S.A. 89*, 8210–8214.
Plateau, P., & Gueron, M. (1982) *J. Am. Chem. Soc. 104*, 7310–7311.
Ptitsyn, O. B., & Finkelstein, A. V. (1983) *Biopolymers 22*, 15–25.
Rance, M., Sorenson, O. W., Bodenhausen, G., Wagner, G., Ernst, R. R., & Wüthrich, K. (1983) *Biochem. Biophys. Res. Commun. 117*, 479–485.
Rizo, J., Blanco, F. J., Kobe, B., Bruch, M. D., & Gierasch, L. M. (1993) *Biochemistry 32*, 4881–4894.
Rooman, M. J., Kocher, J.-P. A., & Wodak, S. J. (1992) *Biochemistry 31*, 10226–10238.
Schwyzer, R. (1987) *EMBO J. 6*, 2255–2259.
Shin, H.-C., Merutkas, G., Waltho, J. P., Wright, P. E., & Dyson, J. H. (1993) *Biochemistry 32*, 6348–6355.
Sönnichsen, F. D., van Eyk, J. E., Hodges, R. S., and Sykes, B. D. (1992) *Biochemistry 31*, 8790–8798.
Sumner, S., Gallagher, K. S., Davis, D. G., Covell, D. G., Jernigan, R. L., & Ferretti, J. A. (1990) *J. Biomol. Struct. Dyn. 8*, 687–707.
Sundaralingam, M., & Sekharudu, Y. C. (1989) *Science 244*, 1333–1337.
Tirado-Rives, J., & Jorgensen, W. L. (1991) *Biochemistry 30*, 3864–3871.
Woody, R. W. (1985) *The Peptides* (Hruby, V., Ed.) Vol. 7, Academic Press, New York.
Woolley, G. A., & Deber, C. M. (1987) *Biopolymers 26*, S109–S121.
Wu, C., & Yang, J. T. (1978) *Biochem. Biophys. Res. Commun. 82*, 85–91.
Wu, C., & Yang, J. T. (1983) *Biochim. Biophys. Acta 746*, 72–80.
Wu, C., Hachimori, A., & Yang, J. T. (1982) *Biochemistry 21*, 4556–4562.
Wüthrich, K. (1986) *NMR of Proteins and Nucleic Acids*, John Wiley and Sons, New York.
Wüthrich, K., Billeter, M., & Brown, W. (1983) *J. Mol. Biol. 169*, 949–961.
Yang, J. T., Wu, C.-S. C., & Martinez, H. M. (1986) *Methods Enzymol. 130*, 208–269.
Yu, C., & Yang, T.-H. (1991) *J. Chin. Biochem. Soc. 20*, 99–105.